NGVLA Memo 127: A Comparison of the Imaging Capabilities of RevF and RevE ngVLA Configurations for Protoplanetary Disk Studies

A. A. Papazyan[1], L. Ricci[1,*]

[1] *Department of Physics and Astronomy, California State University Northridge, 18111 Nordhoff Street, Northridge, CA 91330, USA*

[*] *Corresponding author: Luca Ricci, luca.ricci@csun.edu*

In this report we compare the imaging performance of two antenna configurations recently considered for the ngVLA, i.e. RevE and RevF, for observations of the protoplanetary disk model presented in Zhang et al. (2018), Harter et al. (2020) and Burrill et al. (2022). The model calculates the evolution of a disk with gas and dust which is perturbed gravitationally by a planet at 3 au from the star and with a planet-to-star mass ratio of 1 $M_{\oplus}/M_{\odot}$, representing for example an Earth-mass planet orbiting a 1 $M_{\odot}$ star. The disk has an initial gas surface density of 300 g/cm^2 and dust-to-gas mass ratio of 0.01. The gas viscosity in the model is characterized by a low value for the Shakura-Sunyaev parameter $\alpha \approx 10^{-5}$ (Shakura & Sunyaev 1973). For our simulations of the ngVLA observations we considered the dust continuum map of this disk model at a wavelength of $\approx$ 3 mm at a distance of 140 pc. The synthetic model image is presented in Figure 1, and shows the multiple rings and gaps which are the products of the disk-planet interaction in a disk with low gas viscosity.

Harter et al. (2020) presented ngVLA simulated observations for this model using the RevD antenna configuration. In this work we performed simulations using similar methods as described in Ricci et al (2018) and Harter et al. (2020) using more recent designs for the ngVLA antenna configuration, i.e. RevE and RevF (for a description on the differences in the layouts of the two configurations, see ngVLA memo #104). The main goal is to compare the imaging performance of these two proposed antenna configurations in this field of study.

We used the `simobserve`, `setnoise`, and `tclean` tasks in CASA to derive the measurement set visibility file of the model image, perform the Fourier Transform of the visibilities and deconvolve the dirty image to derive the final image. The images presented here are simulated using a Briggs weighting scheme, with the robust parameter set to r = -0.5. Other values of the robust parameter were tested, and we found that the -0.5 value provided the best imaging results for the ring-gap substructures in the disk. Additionally, we ran the `tclean` task for the same measurement set visibility file of the simulated disk model, but applied an outer taper with uv-taper scale of 1 mas. As expected, this increased the overall signal-to-noise ratio in the simulated images, at the cost of a moderate loss in angular resolution. The images obtained without and with outer taper are shown in Figures 2 and 3, respectively. The RevE image without outer

taper has an rms noise value of ≈ 0.234 μJy/beam (evaluated outside of the region with disk emission), and a beam size of 1.41×1.15 mas, whereas the rms noise and beam size for the RevF image are ≈ 0.235 μJy/beam and 1.41×1.15 mas, respectively. For the simulations with the 1 mas uv-taper, the measured rms noise values and beam sizes are ≈ 0.259 μJy/beam and 2.13 x 1.91 mas for revF, and ≈ 0.258 μJy/beam and 2.16 x 1.89 mas for revE, respectively.

As shown in Fig. 2 and 3, both RevF and RevE configurations are able to resolve the primary gap opened by the planet in the disk with or without 1 mas outer taper, although the outer taper image provides better signal-to-noise at the location of the ring-gap substructure. The total flux values we measured from the disk simulations without the 1 mas uv-taper are ≈ 10.9 mJy in both RevF and RevE configurations with a difference slightly below the 1% level. Similar results were obtained for the simulations with the 1 mas outer taper, with a measured total flux in both configurations of ≈ 9.02 mJy.

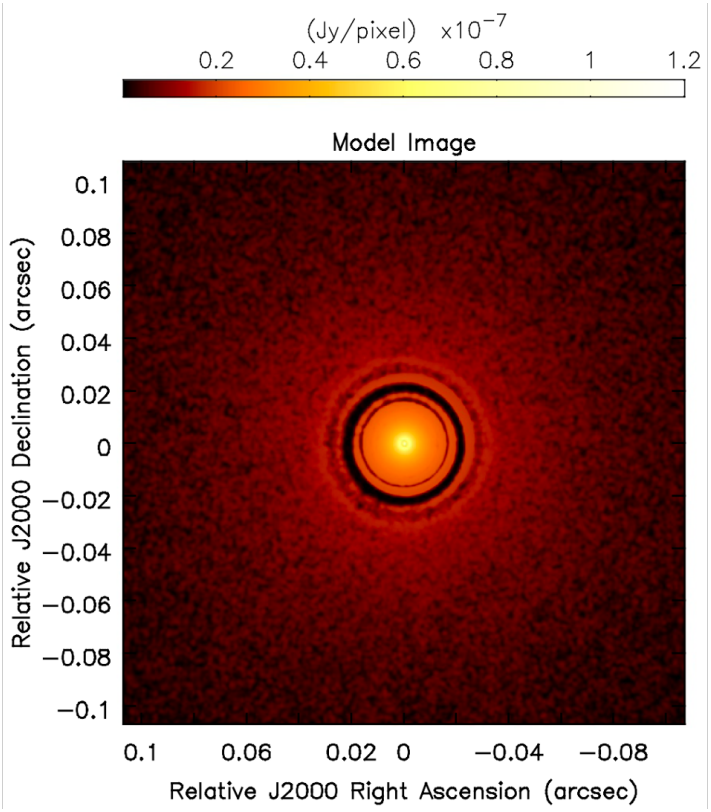

Figure 1. Dust continuum map at $\lambda = 3$mm for the disk model considered in this study.

Figures 4a and 4c present a comparison image between the two simulated images with RevF and revE without and with outer taper, respectively. The pixel values of these comparison images were obtained by first subtracting the pixel values $I(x, y)$ of the RevF and RevE images, and then normalizing it over an average rms noise value of 0.26 μJy/beam, obtained from the revF image: $[I^{\rm RevE}(x, y) - I^{\rm RevF}(x, y)]/\sigma_{\rm RevF}$,

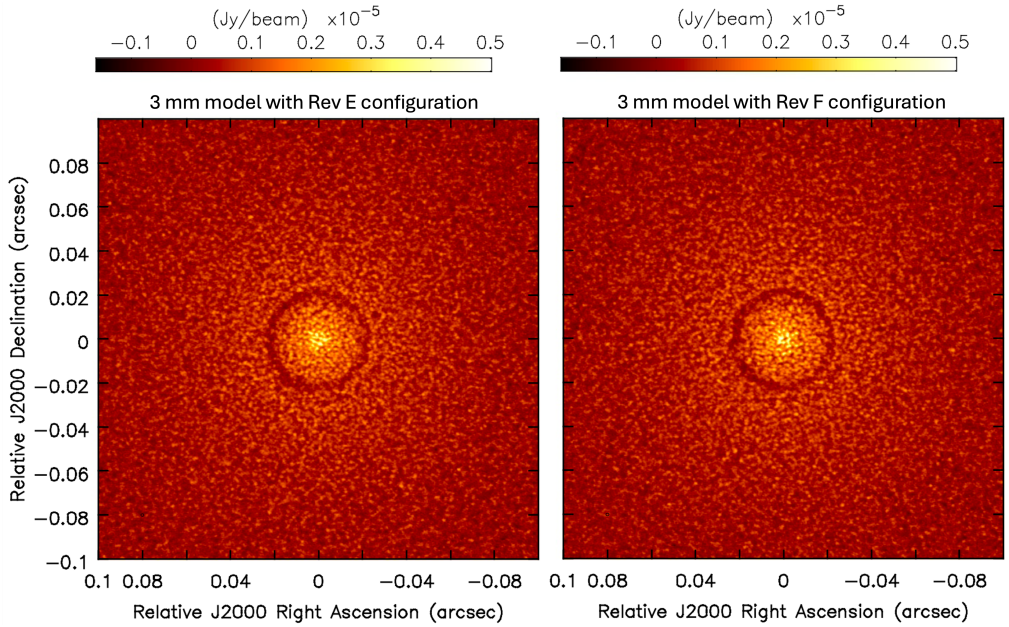

Figure 2. Simulated ngVLA images of the dust continuum emission for the disk model at 3 mm. The left and right images present the simulated observations using the RevE and RevF antenna configurations, respectively.

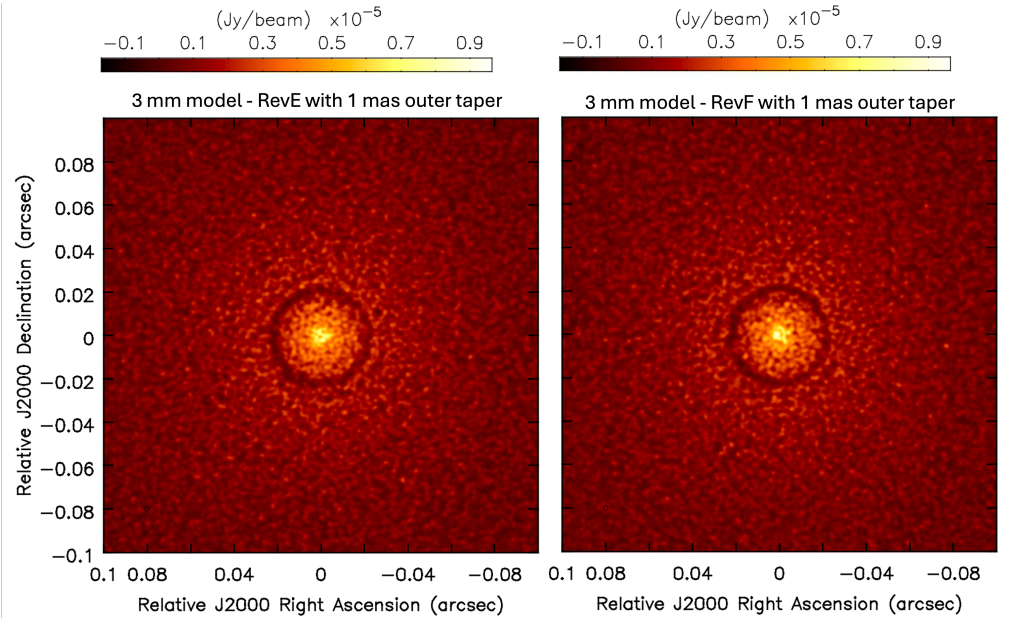

Figure 3. Same as in Figure 2, but with an outer taper with uv-scale of 1 mas applied during the imaging process.

where $\sigma_{\rm RevF}$ is the rms noise measured in the revF image. Figures 4b and 4d present the corresponding histograms for the pixel values of the comparison images shown

in Figures 4a and 4c, respectively. Both the median and mean of the pixel values of the comparison images are consistent with 0 at the $< 0.3\%$ level in either case with or without outer taper. The comparison images and the histograms show that the two configurations produce very similar images.

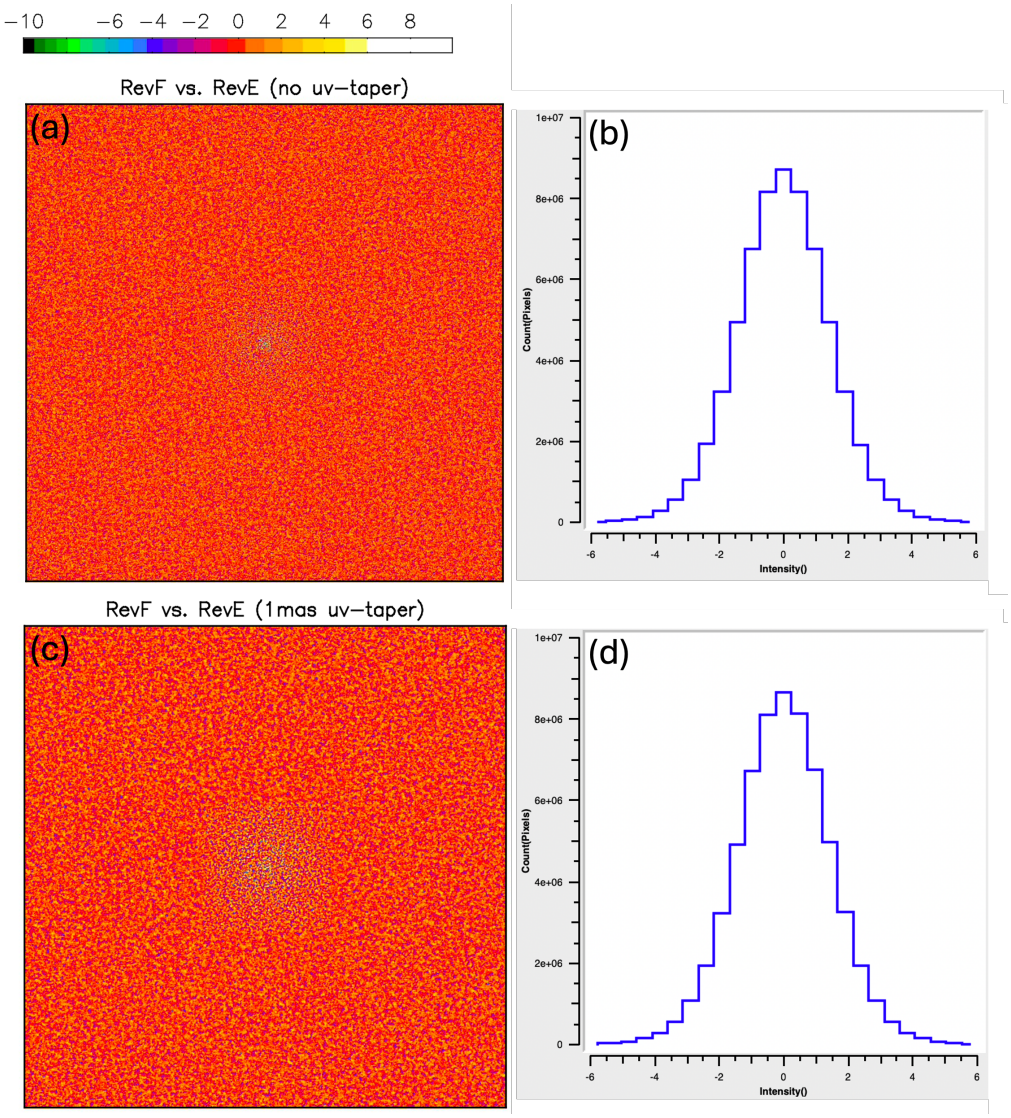

Figure 4. Panels a) and c) Comparison images between RevF and RevE as defined in the text, without and with outer taper, respectively; panels b) and d) Corresponding histograms for the pixel values of the two comparison images shown on the left.

References

Burrill, B., Ricci, L., Harter, S. K. et al. 2022, ApJ 928, 40
Harter, S. K., Ricci, L., Zhang, S., Zhu, Z. 2020, ApJ 905, 24

Ricci, L., Liu, S.-F., Isella, Andrea; Li, H. 2018, ApJ 853, 110
Shakura, N. I., & Sunyaev, R. A. 1973, A&A, 500, 33
Zhang, S., Zhu, Z., Huang, J., et al. 2018, ApJL, 869, L47